1   **Chronic infection of adult zebrafish with rough or smooth variant *Mycobacterium abscessus***

2   **causes necrotising inflammation and differential activation of host immunity**

3

4   Elinor Hortle[1,2]*, Julia Y Kam[1]*, Elizabeth Krogman[1]*, Sherridan E Warner[1,2], Pradeep

5   Manuneedhi Cholan[1], Kazu Kikuchi[3,4], James A Triccas[2], Warwick J Britton[1,2], Matt D Johansen[5],

6   Laurent Kremer[5,6], Stefan H Oehlers[1,2#]

7

8   1 Tuberculosis Research Program at Centenary Institute, The University of Sydney, Camperdown

9   NSW Australia

10   2 The University of Sydney, Faculty of Medicine and Health & Marie Bashir Institute,

11   Camperdown NSW Australia

12   3 Developmental and Stem Cell Biology Division, Victor Chang Cardiac Research Institute,

13   Darlinghurst, NSW Australia

14   4 St. Vincent's Clinical School, University of New South Wales, Kensington, NSW 2052, Australia

15   5 Centre National de la Recherche Scientifique UMR 9004, Institut de Recherche en Infectiologie

16   de Montpellier (IRIM), Université de Montpellier, 1919 Route de Mende, 34293, Montpellier,

17   France.

18   6 INSERM, IRIM, 34293 Montpellier, France.

19

20   *These authors contributed equally and are listed in alphabetical order.

21

22   [#] Corresponding author: Dr Stefan Oehlers, stefan.oehlers@sydney.edu.au

23

30

31   Keywords: non-tuberculous mycobacterium, rapid-growing mycobacteria, animal model, zebrafish,

32   glycopeptidolipids

33

34   **Abstract**

35 Infections caused by *Mycobacterium abscessus* are increasing in prevalence within patient groups

36 with respiratory comorbidities including Cystic Fibrosis or Chronic Obstructive Pulmonary Disease.

37 Initial colonisation by the smooth colony *M. abscessus* (S) can be followed by an irreversible

38 genetic switch into a highly inflammatory rough colony *M. abscessus* (R), often associated with a

39 decline in pulmonary function. Currently available animal models such as the embryonic zebrafish,

40 have largely explored the role of innate immunity in the pathogenesis of *M. abscessus*, and

41 demonstrated that infection with the R variant produces a hyperinflammatory infection due to the

42 presence of large extracellular cords, whereas the S variant produces a chronic persistent infection.

43 However, our understanding of the role of adaptive immunity in *M. abscessus* pathogenesis is

44 largely unknown. Here, we have used intraperitoneal infection of adult zebrafish to model *M.*

45 *abscessus* pathogenesis in the context of fully functioning host immunity. We find infection with

46 the R variant penetrates host organs causing an inflammatory immune response leading to necrotic

47 granuloma and abscess formation within 2 weeks. The R bacilli are targeted by T cell-mediated

48 immunity and burden is progressively reduced. Strikingly, the S variant colonises host internal

49 surfaces at high loads and is met with a robust innate immune response. Invasive granuloma

50 formation is delayed in S variant infection compared to R variant infection. In mixed infections, the

51 S variant outcompetes the R variant in an adaptive-immunity dependent manner. We also find the R

52 variant activates innate immunity to detriment of S variant *M. abscessus* in mixed infections. These

53 findings demonstrate the applicability of the adult zebrafish to model persistent *M. abscessus*

54 infection.

55

56 **Introduction**

57 *Mycobacterium abscessus* is an increasingly recognized human pathogen responsible for a wide

58 array of clinical manifestations including muco-cutaneous infections, disseminated or chronic

59 pulmonary diseases. The latter is mostly encountered in patients with underlying lung disorders,

60 such as bronchiectasis or cystic fibrosis (CF). Irrespective of being a rapid-growing mycobacteria

61 (RGM), *M. abscessus* displays many pathophysiological traits with slow-growing mycobacteria

62 (SGM), such as *Mycobacterium tuberculosis*. These include the capacity to persist silently within

63 granulomatous structures and to produce pulmonary caseous lesions (1, 2). In addition, *M.*

64 *abscessus* is notorious for being one of the most-drug resistant mycobacterial species, characterized

65 by a wide panel of acquired and innate drug resistance mechanisms against nearly all anti-tubercular

66 drugs, as well as many classes of antibiotics (3). Consequently, this explains the complexity and

67 duration of the treatments and the high level of therapeutic failure (4).

68   *M. abscessus* exists either as a smooth (S) or a rough (R) colony morphotype associated with

69 distinct clinical outcomes (5). Previous epidemiological studies have highlighted the association of

70   the R variant, persisting for many years in the infected host, with a rapid decline in the pulmonary

71   functions (6-8). It is well established that these morphological differences between S and R variants

72   are dependent on the presence or absence of surface-exposed glycopeptidolipids (GPL),

73   respectively (5, 9, 10). However, our knowledge of the pathophysiological characteristics and

74   interactions between R or S variants with the host immune cells remains largely incomplete and is

75   hampered by the lack of animal models that are permissive to persistent *M. abscessus* infection.

76   Intravenous injection or aerosol administration of *M. abscessus* in immunocompetent BALB/c

77   mice fails to establish a persistent infection, typified by a rapid clearance of the bacilli from the

78   liver, spleen and lungs within 4 weeks (11). Immunosuppression is required to produce a

79   progressive high level of infection with *M. abscessus* in mice, as shown in nude, SCID (severe

80   combined immunodeficiency), interferon-gamma (GKO) and granulocyte-macrophage colony-

81   stimulating factor (GM-CSF) knock-out mice (12).

82   The contribution of B and T cells in the control of *M. abscessus* infection has been studied in

83   C57BL/6 mice with $Rag2^{-/-}$, $Cd3e^{-/-}$ and $\mu MT^{-/-}$ knockouts. These studies indicated that infection

84   control was primarily T cell dependent in the spleen, and both B and T cell dependent in the liver

85   (13). In addition, IFNg-receptor KO mice ($ifngr1^{-/-}$) were significantly impaired in their control of

86   *M. abscessus* both in the spleen and in the liver, with markedly different granulomas and more

87   pronounced in $TNF^{-/-}$ mice (13). This points to the central role of T-cell immunity, IFNg and TNF

88   for the control of *M. abscessus* in C57BL/6 mice, similarly to the control of *M. tuberculosis*

89   infection.

90   In recent years, alternative non-mammalian models, such as Drosophila (14), Galleria larvae

91   (15), and zebrafish embryos (16) have been developed to study the chronology and pathology of *M.*

92   *abscessus* infection and for *in vivo* therapeutic assessment of drugs active against *M. abscessus*. In

93   particular, zebrafish embryos have delivered important insights into the pathogenesis of *M.*

94   *abscessus* and the participation of innate immunity in controlling infection. The optical

95   transparency of zebrafish embryos has been used to visualise the formation of large extracellular

96   cords by the R form *in vivo*, representing a mechanism of immune subversion by preventing

97   phagocytic destruction and highlighting the importance bacterial virulence factors such as the

98   dehydratase MAB_4780 and the $MmpL8_{MAB}$ lipid transporter (9, 17, 18). Other studies in zebrafish

99   embryos have demonstrated the contribution of host TNF signalling and IL8-mediated neutrophil

100 recruitment for protective granulomatous immunity against *M. abscessus* (19), and the link

101 between dysfunctional CFTR and vulnerability to *M. abscessus* infection via the macrophage

102 oxidative response (20).

103 Adult zebrafish models have been well-described for the study of mycobacterial pathogenesis

104 by *Mycobacterium marinum*, used as a surrogate for the closely related *M. tuberculosis*, and the

3

105   human pathogen *Mycobacterium leprae* (21-23). Encompassing a fully functional immune system,

106   previous studies in adult zebrafish with pathogenic mycobacteria such as *M. marinum* have

107   unravelled the interplay between innate and adaptive immunity in mycobacterial granuloma

108   formation and function.

109   Herein, we addressed whether adult zebrafish may be a useful host to analyse and compare

110   the chronology of infection with *M. abscessus* S and R variants and to study the contribution of the

111   T cell-mediated immunity and granulomatous response in *M. abscessus* infection.

112

113   **Results**

114   <u>Adult zebrafish can be chronically infected with *M. abscessus.*</u>

115   To establish the susceptibility of adult zebrafish to infection by *M. abscessus*, we performed a dose

116   escalation experiment up to 10^6 CFU per animal with the rough (R) and smooth (S) variants of the

117   reference strain CIP104536^T. While animals underwent a period of sickness behaviour within the

118   first week of infection, we did not observe mortality for up to 4 weeks post infection (wpi) (data not

119   shown). To determine if *M. abscessus* produces a persistent infection in adult zebrafish, we

120   performed CFU recovery on animals infected with a standard dose of 10^5 CFU (Figure 1A). We

121   observed a progressive clearance of the R variant with a 1-log reduction in burden from 1 day post

122   infection (dpi) to 4 wpi (P=0.018). Conversely, the S variant was recovered at a consistent burden

123   across the 4 week duration of the experiment (1 dpi vs 4 wpi, P=0.12). We hypothesised that the

124   better survival of the S variant compared to the R variant could be attributed to reduced

125   immunogenicity of the CIP104536 S cell surface and different modes of growth in macrophages

126   (24). To test this hypothesis, we performed qPCR detection of zebrafish immune gene expression

127   from infected adult homogenates (25). We observed higher innate immunity-associated *il1b*

128   transcription in the *M. abscessus* S-infected group from early in infection and a late trend to

129   increases in *il1b* transcription in 4 wpi *M. abscessus* R-infected animals (Figure 1B). Expression of

130   *cd3*, indicative of total T cell numbers, was significantly decreased in all *M. abscessus*-infected

131   animals at 2 wpi but returned to uninfected levels by 4 wpi with higher *cd3* expression in *M.*

132   *abscessus* R-infected compared to *M. abscessus* S-infected animals (Figure 1C). There was a trend

133   towards increased transcription of the Th1 activation marker *ifng* in R compared to S or uninfected

134   fish at 4 wpi (Figure 1D).

135

136   <u>Adult zebrafish contain *M. abscessus* R within granulomas.</u>

137   We next performed histology on adult zebrafish infected with fluorescent *M. abscessus* R. At 3 dpi,

138   bacteria were diffusely spread through the peritoneal cavity with occasional foci of infection located

139   external to peritoneal organs. From 10 dpi to 2 wpi we noted a heterogeneous mix of unorganised

140   lesions (Figure 2A) and organised lesions with stereotypical concentric rings of nuclei around a
141   central focus of bacteria and necrotic debris in all animals (Figure 2B). We also observed the
142   appearance of very large abscess-like granulomas filled with fluorescent bacteria and necrotic
143   debris measuring over 600 µm at a rate of no more than 1 per infected animal from 2 wpi onwards
144   (Figure 2C). Oil red O staining revealed the accumulation of foam cells in cellular rim of *M.*
145   *abscessus* R granulomas (Figure 2D), consistent with immunopathology seen in
146   immunocompromised mice infected with *M. abscessus* (12). Although we observed a fairly stable
147   proportion of organised granulomas in *M. abscessus* R-infected adult zebrafish from 10 to 28 dpi
148   (Figure 2E), the proportion of fluorescent bacteria associated with organised granulomas
149   significantly increased from 10 to 28 dpi corresponding to the appearance of abscesses at 14 dpi
150   (Figure 2F).

151

152   <u>Adult zebrafish contain *M. abscessus* S infection prior to delayed granuloma formation.</u>
153   Histological analysis of adult zebrafish infected with fluorescent *M. abscessus* S revealed
154   significantly less tissue damage than the equivalent *M. abscessus* R infection up to 2 wpi. *M.*
155   *abscessus* S was observed to grow freely in mesenteric spaces and form poorly organised cellular
156   granulomas at 2 wpi (Figure 3A). We observed the appearance of tissue-invasive organised
157   granulomas at 4 wpi (Figure 3B). Although these granulomas could reach similar size to the very
158   large abscess-like granulomas seen in *M. abscessus* R infection, there was little Oil Red O staining
159   in *M. abscessus* S granulomas indicating a lack of foam cell formation (Figure 3C).
160   We observed a significant increase in the proportion of organised granulomas in S-infected
161   adult zebrafish from 2 to 4 wpi (Figure 3D). Similarly, the proportion of fluorescent bacteria
162   associated with organised granulomas significantly also increased from 2 to 4 wpi corresponding to
163   the consolidation of *M. abscessus* S into granulomas (Figure 3E).
164   The cytokine *tumour necrosis factor* (*tnf*) is essential for the containment of *M. abscessus* in
165   zebrafish embryos (19). We next took advantage of the progressive pathology observed in 4 wpi *M.*
166   *abscessus* S-infected *TgBAC(tnfa:GFP)*[pd1028] animals, where GFP expression is driven by the *tnfa*
167   promoter, to investigate if *tnf* expression is linked to granuloma formation. Expression of GFP was
168   concentrated to tightly organised necrotic granulomas demonstrating a conserved induction of *tnf*
169   expression during *M. abscessus* granuloma formation in adult zebrafish (Figure 3F).

170

171   <u>Adaptive immunity is necessary for control of *M. abscessus* infection in adult zebrafish.</u>
172   Given the requirement for T cells to maintain granuloma structure in adult zebrafish *M. marinum*
173   infection (23), we next asked if there was T cell involvement around *M. abscessus* granulomas
174   using the recently described *TgBAC(lck:GFP)*[vcc4] zebrafish line (23, 26). We observed T cell

5

175   association and penetration throughout unorganised and organised *M. abscessus* R granulomas, but

176   T cells were largely excluded from the cores of the very large abscess-like lesions (Figure 4A).

177   Conversely, we did not observe T cell interaction with *M. abscessus* S growing around peritoneal

178   organs until invasive granuloma formation after 2 wpi, which was indistinguishable from the T cell

179   response to *M. abscessus* R infection (Figure 4B). To directly test the requirement of T cells in

180   containing *M. abscessus* we next utilised the *lck*$^{-/-sa410}$ mutant line which is T cell-deficient. We

181   infected wild type (WT) control and *lck*$^{-/-sa410}$ mutant adult zebrafish with both the S and R variants.

182   T cell-deficient adult zebrafish were significantly more susceptible to *M. abscessus* R infection with

183   reduced survival over 4 weeks of infection (P = 0.0005, Log-rank test) (Figure 4C). T cell

184   deficiency had a less pronounced effect on the survival of animals infected with *M. abscessus* S

185   compared to *M. abscessus* R infection (WT S vs lck-/- S P = 0.03, Log-rank test), although both

186   groups eventually succumbed to infection at the same rate after 5 wpi (P = 0.78, Log-rank test)

187   (Figure 4C). Consequently, bacterial burden was significantly increased in 2 wpi *lck*$^{-/-sa410}$ mutants

188   infected with the R (Figure 4D), but not the S variant (Figure 4E). These observations confirm the

189   highly inflammatory nature of *M. abscessus* R infection is conserved in the adult zebrafish model

190   and mediated by T-cells. Conversely, colonisation by *M. abscessus* S is contained by sufficient

191   activation of the innate immune response until invasive infection between 2 and 4 wpi.

192

193   *M. abscessus* S has a survival advantage over *M. abscessus* R.

194   To examine our hypothesis that *M. abscessus* S has a survival advantage over *M. abscessus* R in the

195   adult zebrafish infection model, we performed co-infection of adult zebrafish with equal numbers of

196   each variant expressing either Wasabi or Tdtomato fluorescent proteins to enable simple tracking

197   (Figure 5A). Analysis of the ratio of R:S colonies recovered revealed a clear and rapid shift in

198   population proportions from 1:1 at 1 dpi to 0.5 rough:1 smooth ratio that remained stable at 2 wpi

199   (Figure 5B). Coinfection did not affect the progressive reduction in *M. abscessus* R burden as near

200   identical *M. abscessus* R CFUs were recovered from single and mixed-infected animals at 1 and 2

201   wpi (Figure 5C). Coinfection did cause a decrease in the number of recoverable *M. abscessus* S that

202   was not observed in single variant infections at 1 and 2 wpi demonstrating a negative effect of R

203   granuloma formation on the survival of *M. abscessus* S (Figure 5C). Whole mount and histological

204   examination of bacterial distribution in animals infected with *M. abscessus* R expressing Wasabi

205   and *M. abscessus* S expressing Tdtomato revealed co-mingling of S and R variants within

206   granulomas (Figure 5D).

207   We hypothesised that the T cell response induced by the R variant to antigens shared with

208   the S strain could be responsible for the clearance of S strain in mixed infections. To test this

209   hypothesis we infected T-cell deficient *lck*$^{-/-sa410}$ mutant animals with a mixed infection of R and S

210 variants of *M. abscessus*. CFU recovery from these mixed infections in the T-cell deficient animals

211 revealed a similar decrease in *M. abscessus* S burden as observed in WT animals (Figure 5E).

212 Therefore the clearance of *M. abscessus* S strain is mediated by innate immune mechanisms.

213 Interestingly, $lck^{-/-sa410}$ zebrafish had a higher proportion of rough to smooth than in comparable WT

214 animals, confirming the importance of the adaptive immune response for controlling *M. abscessus*

215 R strain burden (Figure 5F).

216

217 **Discussion**

218 In this study, we report for the use of adult zebrafish to probe both host and mycobacterial

219 determinants of pathogenesis during persistent infection with *M. abscessus*. Infection with the R

220 and S variants was maintained over months of infection in genetically intact animals, a major

221 improvement on existing mouse models of *M. abscessus* infection.

222   While the R variant induces a more robust and aggressive infection than the S morphotype in

223 zebrafish embryos (9), this appears to not the case in the adult fish. We observed better clearance of

224 the R variant and establishment of a higher burden of persistent infection with the S variant. One

225 possible explanation for the better survival of the S compared to the R is that, in the presence of

226 effective adaptive immunity, R infection is better controlled due to the induction of a potent Th1

227 cell-mediated response, as evidenced by the increased expression of the CD3 marker and IFN-

228 gamma response at later time points. This contribution of the T cell response was further

229 substantiated using T cell-deficient fish, where infection of $lck^{-/-}$ fish with the R bacilli resulted in a

230 higher bacterial burden than in WT fish, which was not observed with S bacilli. These observations

231 provide insight into the clinical observation that AIDS patients are not at increased risk of *M.*

232 *abscessus* infection to the same degree that AIDS is a risk factor for *M. tuberculosis* and other non-

233 tuberculous mycobacterium infections such as *Mycobacterium avium*.

234   It is well known that the intracellular lifestyle of S and R *M. abscessus* variants differ

235 significantly, resulting in entirely distinct infection scenarios (27). The absence of GPL on the outer

236 mycomembrane causes corded growth of R variants, resulting in multiple bacilli being

237 simultaneously phagocytosed by macrophages and overloaded phagosomes that rapidly activate

238 autophagy pathways (27). Comparatively, the S variant is able to survive for an extended period of

239 time within the phagosome, producing a chronic and persistent infection (28, 29). As such, these

240 polar infection responses may explain why the R displays increased granuloma formation at 2 wpi,

241 compared to S which shows a significantly delayed onset of granuloma formation. Moreover, this

242 observation matches the superior *in vivo* growth performance of S bacilli compared to R (Fig 1A),

243 suggesting that the R variant is at an overall disadvantage because of its intrinsic hyper-

244 inflammatory status and the activation of effective adaptive immunity that results in granuloma

7

245 formation. Taken together, our data provides additional evidence for the distinct intracellular fates

246 of both S and R variants *in vivo*, and further implicates the role of adaptive immunity in granuloma

247 formation and control of *M. abscessus* infection in an adult zebrafish model.

248 Our qPCR analysis surprisingly demonstrated that the S variant elicits greater production of

249 *il1b*; a key inflammatory cytokine, during the first 2 wpi compared to the R variant (Fig 1B). It is

250 likely that this observation is the nett effect of progressive increase in bacterial burden of S variants

251 over time, coupled with the presence of extracellular bacilli and unorganised granuloma formation

252 observed at 2 wpi, compared to the containment and clearance of the R variant in organised

253 granulomas.

254 T cells are critical host determinants in the control of mycobacterial infection (30).

255 Recruitment of T cells into granulomas are thought to be essential in containing persistent infection,

256 while T cell deficiencies are associated with greater mycobacterial infection severities (21, 30-32).

257 Recently, an adult zebrafish infection model for *M. leprae* demonstrated that T cells are essential

258 for containment of infection (29). We examined the recruitment of T cells within granulomas and

259 identified that S variant granulomas were marked by the absence of T cell infiltration at 2 wpi,

260 highlighting the fact that T cells may play a less significant role in S variant infections than those

261 with R variants. Using the $lck^{-/-}$ mutants, we have shown that adult zebrafish are highly susceptible

262 to *M. abscessus* infection and succumb to intraperitoneal infection within 40 days in the absence of

263 T cells, irrespective of bacterial morphotype. Importantly, the R variant displayed an improved *in*

264 *vivo* growth performance in the absence of T cells when compared to wild-type zebrafish,

265 highlighting the role of T cells in the control of R variants. However, this observation was not

266 maintained with the S variant, which showed no increase in bacterial growth *in vivo* irrespective of

267 the absence of T cells early in infection.

268 Our co-infection experiments further support the theory that tissue destruction caused by R

269 variant activates protective trans-acting host innate immunity that impairs bacterial growth, thereby

270 restricting S growth (Graphical Abstract). This suggests *M. abscessus* must balance the benefits of

271 R variant pathogenicity allowing individuals to kill and escape macrophage containment, with the

272 need to avoid activation of host-protective immunity at a population level.

273 To date, our understanding of the diverse immune responses between S and R variants have

274 only been thoroughly described with respect to innate immunity, and currently our knowledge

275 pertaining to adaptive immunity in *M. abscessus* infection has been poorly characterised. Using this

276 new adult zebrafish *M. abscessus* infection model, we have shown that S and R variants produce

277 strikingly different disease phenotypes, which was further exemplified in the absence of a

278 functioning adaptive immune response. Consequently, these results suggest that the host-pathogen

279 interactions dictating *M. abscessus* pathogenesis are complex and may implicate adaptive immunity

280 to a greater extent than originally anticipated. Future work should exploit this new animal model in

281 combination with zebrafish lacking the Cystic fibrosis transmembrane conductance regulator gene,

282 and for the development and testing of novel antibiotics and vaccine candidates that may be used

283 for the treatment of *M. abscessus* infection.

284

285 **Methods**

286 Zebrafish strains and handling

287 Zebrafish strains used in this study are AB strain wildtype, $TgBAC(tnfa:GFP)^{pd1028}$,

288 $TgBAC(lck:EGFP)^{vcc4}$, $lck-/-^{sa410}$ (26, 33). Animals were held in a 28°C incubator with a 14:10 hour

289 light:dark cycle. Animals were infected by intraperitoneal injection with approximately 10^5 CFU *M.*

290 *abscessus*, unless otherwise stated, using a 31 G insulin needle and syringe as previously described

291 (34). Infected zebrafish were recovered into system water and held in 1 L beakers with daily

292 feeding for the duration of the experiment. Infection experiments were carried out with ethical

293 approval from the Sydney Local Health District Animal Welfare Committee approval 16-037.

294

295 *M. abscessus* strains and handling

296 Rough (R) and smooth (S) variants of *M. abscessus* strain CIP104536^T were grown at 30°C in

297 Middlebrook 7H9 broth supplemented with 10% Oleic acid/Albumin/Dextrose/Catalase (OADC)

298 enrichment and 0.05% Tween 80 or on Middlebrook 7H10 agar containing 10% OADC (7H10

299 OADC). Recombinant *M. abscessus* strains expressing Tdtomato or Wasabi were grown in the

300 presence of 500 µg/ml hygromycin (9, 19). Homogenous bacterial suspensions for intraperitoneal

301 injection in adult fish were prepared as previously reported (35).

302

303 Bacterial recovery

304 Animals were euthanised by tricaine anaesthetic overdose and rinsed in sterile water. Individual

305 carcasses were homogenised and serially diluted into sterile water. Homogenates were plated onto

306 7H10 OADC supplemented with 300 µg/ml hygromycin. Plates were grown for at least 4 days at 37

307 degrees.

308

309 Zebrafish and *M. abscessus* gene expression analysis by qPCR

310 RNA was extracted from whole fish homogenates and was reverse transcribed with the Applied

311 Biosystems High Capacity cDNA kit and qPCR was carried out on an Agilent Technologies

312 Stratagene Mx3005P. Zebrafish gene expression primers were previously described by Hammaren

313 *et al.* (25).

314

Histology

315 Animals subjected to cryosectioning as previously described (34). Briefly, euthanasia was

316 performed by tricaine anaesthetic overdose and specimens were fixed for 2-4 days in 10% neutral

317 buffered formalin at 4°. Specimens were then rinsed in PBS, incubated overnight in 30% sucrose,

318 incubated overnight in 50/50 30% sucrose and OCT, and finally incubated overnight in OCT prior

319 to freezing at -80°. Cryosectioning was performed to produce 20 µm thick sections. Sections were

320 post-fixed for 1-2 minutes in 10% neutral buffered formalin and rinsed in PBS prior to further

321 processing. Slides for fluorescent imaging were mounted with coverslips using Fluoromount G

322 containing DAPI. Oil Red O staining was performed as previously described (34, 36). T cells were

323 detected in sections from *TgBAC(lck:GFP)^{vcc4}* zebrafish by anti-GFP staining (primary antibody:

324 ab13970, Abcam; secondary antibody: ab150173, Abcam), stained slides were then mounted with

325 coverslips using Fluoromount G containing DAPI. All imaging was carried out on a Leica

326 DM6000B microscope.

Statistics

330 All statistical testing was carried out using Graphpad Prism. Each data point indicates a single

331 animal unless otherwise stated.

Acknowledgements

References

345 1. H. Medjahed, J. L. Gaillard, J. M. Reyrat, Mycobacterium abscessus: a new player in the

346   mycobacterial field. *Trends Microbiol* **18**, 117-123 (2010).

347 2. J. F. Tomashefski, Jr., R. C. Stern, C. A. Demko, C. F. Doershuk, Nontuberculous

348   mycobacteria in cystic fibrosis. An autopsy study. *Am J Respir Crit Care Med* **154**, 523-528

349   (1996).

350   3.   R. Nessar, E. Cambau, J. M. Reyrat, A. Murray, B. Gicquel, Mycobacterium abscessus: a new
351   antibiotic nightmare. *The Journal of antimicrobial chemotherapy* **67**, 810-818 (2012).

352   4.   B. E. Ferro *et al.*, Failure of the Amikacin, Cefoxitin, and Clarithromycin Combination
353   Regimen for Treating Pulmonary Mycobacterium abscessus Infection. *Antimicrob Agents*
354   *Chemother* **60**, 6374-6376 (2016).

355   5.   S. T. Howard *et al.*, Spontaneous reversion of Mycobacterium abscessus from a smooth to a
356   rough morphotype is associated with reduced expression of glycopeptidolipid and
357   reacquisition of an invasive phenotype. *Microbiology* **152**, 1581-1590 (2006).

358   6.   E. Catherinot *et al.*, Acute respiratory failure involving an R variant of Mycobacterium
359   abscessus. *J Clin Microbiol* **47**, 271-274 (2009).

360   7.   C. R. Esther, Jr., D. A. Esserman, P. Gilligan, A. Kerr, P. G. Noone, Chronic Mycobacterium
361   abscessus infection and lung function decline in cystic fibrosis. *J Cyst Fibros* **9**, 117-123
362   (2010).

363   8.   B. E. Jonsson *et al.*, Molecular epidemiology of Mycobacterium abscessus, with focus on
364   cystic fibrosis. *J Clin Microbiol* **45**, 1497-1504 (2007).

365   9.   A. Bernut *et al.*, Mycobacterium abscessus cording prevents phagocytosis and promotes
366   abscess formation. *Proc Natl Acad Sci U S A* **111**, E943-952 (2014).

367   10.   H. Medjahed, J. M. Reyrat, Construction of Mycobacterium abscessus defined
368   glycopeptidolipid mutants: comparison of genetic tools. *Appl Environ Microbiol* **75**, 1331-
369   1338 (2009).

370   11.   A. Bernut *et al.*, In vivo assessment of drug efficacy against Mycobacterium abscessus using
371   the embryonic zebrafish test system. *Antimicrob Agents Chemother* **58**, 4054-4063 (2014).

372   12.   A. Obregon-Henao *et al.*, Susceptibility of Mycobacterium abscessus to antimycobacterial
373   drugs in preclinical models. *Antimicrob Agents Chemother* **59**, 6904-6912 (2015).

374   13.   M. Rottman *et al.*, Importance of T cells, gamma interferon, and tumor necrosis factor in
375   immune control of the rapid grower Mycobacterium abscessus in C57BL/6 mice. *Infect*
376   *Immun* **75**, 5898-5907 (2007).

377   14.   C. T. Oh, C. Moon, M. S. Jeong, S. H. Kwon, J. Jang, Drosophila melanogaster model for
378   Mycobacterium abscessus infection. *Microbes Infect* **15**, 788-795 (2013).

379   15.   M. Meir, T. Grosfeld, D. Barkan, Establishment and Validation of Galleria mellonella as a
380   Novel Model Organism To Study Mycobacterium abscessus Infection, Pathogenesis, and
381   Treatment. *Antimicrob Agents Chemother* **62** (2018).

382   16.   A. Bernut, J. L. Herrmann, D. Ordway, L. Kremer, The Diverse Cellular and Animal Models
383   to Decipher the Physiopathological Traits of Mycobacterium abscessus Infection. *Front Cell*
384   *Infect Microbiol* **7**, 100 (2017).

11

385   17.   V. Dubois *et al.*, MmpL8MAB controls Mycobacterium abscessus virulence and production
386   of a previously unknown glycolipid family. *Proc Natl Acad Sci U S A* **115**, E10147-E10156
387   (2018).

388   18.   I. Halloum *et al.*, Deletion of a dehydratase important for intracellular growth and cording
389   renders rough Mycobacterium abscessus avirulent. *Proc Natl Acad Sci U S A* **113**, E4228-
390   4237 (2016).

391   19.   A. Bernut *et al.*, Mycobacterium abscessus-Induced Granuloma Formation Is Strictly
392   Dependent on TNF Signaling and Neutrophil Trafficking. *PLoS Pathog* **12**, e1005986 (2016).

393   20.   A. Bernut *et al.*, CFTR Protects against Mycobacterium abscessus Infection by Fine-Tuning
394   Host Oxidative Defenses. *Cell reports* **26**, 1828-1840 e1824 (2019).

395   21.   C. A. Madigan, J. Cameron, L. Ramakrishnan, A Zebrafish Model of Mycobacterium leprae
396   Granulomatous Infection. *J Infect Dis* **216**, 776-779 (2017).

397   22.   S. H. Oehlers *et al.*, Interception of host angiogenic signalling limits mycobacterial growth.
398   *Nature* **517**, 612-615 (2015).

399   23.   L. E. Swaim *et al.*, Mycobacterium marinum infection of adult zebrafish causes caseating
400   granulomatous tuberculosis and is moderated by adaptive immunity. *Infect Immun* **74**, 6108-
401   6117 (2006).

402   24.   A. L. Roux *et al.*, The distinct fate of smooth and rough Mycobacterium abscessus variants
403   inside macrophages. *Open Biol* **6** (2016).

404   25.   M. M. Hammaren *et al.*, Adequate th2-type response associates with restricted bacterial
405   growth in latent mycobacterial infection of zebrafish. *PLoS Pathog* **10**, e1004190 (2014).

406   26.   K. Sugimoto, S. P. Hui, D. Z. Sheng, M. Nakayama, K. Kikuchi, Zebrafish FOXP3 is required
407   for the maintenance of immune tolerance. *Dev Comp Immunol* **73**, 156-162 (2017).

408   27.   A.-L. Roux *et al.*, The distinct fate of smooth and rough Mycobacterium abscessus variants
409   inside macrophages. *Open biology* **6** (2016).

410   28.   A. Bernut *et al.*, *Mycobacterium abscessus* cording prevents phagocytosis and promotes
411   abscess formation. *Proceedings of the National Academy of Sciences* **111**, 943-952 (2014).

412   29.   L. Ramakrishnan, Revisiting the role of the granuloma in tuberculosis. *Nature Reviews
413   Immunology* **12**, 352-366 (2012).

414   30.   F. M. Collins, Mycobacterial disease, immunosuppression, and acquired immunodeficiency
415   syndrome. *Clin Microbiol Rev* **2**, 360-377 (1989).

416   31.   T. Mogues, M. E. Goodrich, L. Ryan, R. LaCourse, R. J. North, The relative importance of T
417   cell subsets in immunity and immunopathology of airborne Mycobacterium tuberculosis
418   infection in mice. *J Exp Med* **193**, 271-280 (2001).

419 32. J. D. Yang *et al.*, Mycobacterium tuberculosis-specific CD4+ and CD8+ T cells differ in their
420   capacity to recognize infected macrophages. *PLoS Pathog* **14**, e1007060 (2018).
421 33. L. Marjoram *et al.*, Epigenetic control of intestinal barrier function and inflammation in
422   zebrafish. *Proc Natl Acad Sci U S A* **112**, 2770-2775 (2015).
423 34. T. Cheng, J. Y. Kam, M. D. Johansen, S. H. Oehlers, High content analysis of granuloma
424   histology and neutrophilic inflammation in adult zebrafish infected with Mycobacterium
425   marinum. *Micron* 10.1016/j.micron.2019.102782 (2019).
426 35. A. Bernut *et al.*, Deciphering and Imaging Pathogenesis and Cording of Mycobacterium
427   abscessus in Zebrafish Embryos. *J Vis Exp* 10.3791/53130 (2015).
428 36. M. D. Johansen *et al.*, Mycobacterium marinum infection drives foam cell differentiation in
429   zebrafish infection models. *Dev Comp Immunol* **88**, 169-172 (2018).

430

431 **Figure Legends**

432

433 Figure 1: *M. abscessus* establishes chronic infection in adult zebrafish.

434 A. Enumeration of CFUs from adult zebrafish infected with either the R or the S morphotype of *M.*

435 *abscessus*.

436 B. Gene expression analysis of zebrafish *interleukin 1b*.

437 C. Gene expression analysis of zebrafish *cd3*.

438 D. Gene expression analysis of zebrafish *interferon gamma*.

439 Statistical tests by one-way ANOVA with Tukey's multiple comparisons test. Data is pooled from

440 10 animals across 2 independent experiments.

441

442 Figure 2: *M. abscessus* R infection causes progressive granulomatous pathology.

443 A. Stereotypical unorganised granuloma in a 2 wpi adult zebrafish infected with the R variant of *M.*

444 *abscessus* expressing Tdtomato. Scale bar indicates 100 µm.

445 B. i. Stereotypical organised granuloma in a 2 wpi adult zebrafish infected with R *M. abscessus*-

446 Tdtomato and ii. Higher magnification image of granuloma wall. Arrowheads indicate epithelised

447 macrophage nuclei surrounding the mycobacterial core. Scale bar indicates 100 µm.

448 C. Example of a very large abscess-like granuloma in a 2 wpi adult zebrafish infected with R *M.*

449 *abscessus*-Tdtomato measuring approximately 600 µm in diameter. Scale bar indicates 200 µm.

450 D. Example of Oil Red O-stained very large abscess-like granuloma in a 2 wpi adult zebrafish

451 infected with R *M. abscessus*. Arrowheads indicate Oil Red O-positive foamy macrophages

452 surrounding the mycobacterial core. Scale bar indicates 200 µm.

13

453   E. Quantification of granuloma organisation in adult zebrafish infected with R *M. abscessus*. Data is

454   pooled from 2 animals per timepoint.

455   F. Quantification of bacterial burden stratified by granuloma organisation in adult zebrafish infected

456   with R *M. abscessus*. Data is pooled from 2 animals per timepoint, statistical testing by Chi-squared

457   test.

458

459   Figure 3: *M. abscessus* S infection causes delayed progressive granulomatous pathology.

460   A. Examples S *M. abscessus*-Tdtomato lesions from 2 wpi adult zebrafish. i. *M. abscessus* growing

461   free, external to peritoneal organs. ii and iii. Stereotypical examples of unorganised cellular

462   granulomas around sites of sparse *M. abscessus* infection.

463   B. Stereotypical large granuloma found in 4 wpi adult zebrafish infected with S *M. abscessus*-

464   Tdtomato. Note lack of punctate bacterial fluorescence in the core of the granuloma compared to

465   second granuloma to the right.

466   C. Example of Oil Red O-stained large granuloma in 4 wpi adult zebrafish infected with S *M.*

467   *abscessus*. Note lack of lipid staining in the rim of the granuloma compared to R infection.

468   D. Quantification of granuloma organisation in adult zebrafish infected with S *M. abscessus*. Data is

469   pooled from at least 2 animals per timepoint, statistical testing by Chi-squared test.

470   E. Quantification of bacterial burden stratified by granuloma organisation in adult zebrafish infected

471   with S *M. abscessus*. Data is pooled from at least 2 animals per timepoint, statistical testing by Chi-

472   squared test.

473   F. Example of S *M. abscessus*-Tdtomato lesions in 4 wpi *TgBAC(tnfa:GFP)^{pd1028}* adult zebrafish.

474   Arrowheads indicate organised necrotic granulomas with strong *tnfa* expression marked by GFP.

475   Scale bars indicate 200 μm.

476

477   Figure 4: T cells are necessary to control R but not S *M. abscessus* infection.

478   A. Examples of T cell recruitment to granulomas in 2 wpi *TgBAC*(*lck*:*EGFP*)^{vcc4} adult zebrafish

479   infected with R *M. abscessus*-Tdtomato . i. Example of an unorganised granuloma. ii. Example of

480   an organised granuloma. iii. Example of a very large abscess-like granuloma. Scale bars indicate

481   100 μm.

482   B. Example of lack of T cell recruitment to S *M. abscessus*-Tdtomato in 2 wpi

483   *TgBAC*(*lck*:*EGFP*)^{vcc4} adult zebrafish. Scale bar indicates 100 μm.

484   C. Survival analysis of WT and lck-/- ^{sa410} adult zebrafish infected with R or S *M. abscessus*.

485   D. Enumeration of CFUs from 2 wpi WT and lck-/- ^{sa410} adult zebrafish infected with R *M.*

486   *abscessus*. Statistical testing by T-test.

14

487   E. Enumeration of CFUs from 2 wpi WT and lck-/- ^{sa410} adult zebrafish infected with S *M.*

488   *abscessus*. Statistical testing by T-test.

489

490   Figure 5: S *M. abscessus* has a survival advantage over R *M. abscessus*.

491   A. Schema outlining mixed infection experiment.

492   B. Ratio of R:S CFUs recovered from WT adult zebrafish infected with a mixture of differentially

493   labelled R and S variant *M. abscessus*.

494   C. Enumeration of CFUs from the three groups of WT adult zebrafish outlined in panel A. Data is

495   pooled from two replicates, statistical testing by ANOVA.

496   D. Representative images of granuloma from adult zebrafish infected with a mixture of R

497   expressing Wasabi and S expressing Tdtomato *M. abscessus*.

498   E. Enumeration of CFUs from the three groups of lck-/- ^{sa410} adult zebrafish outlined in panel A.

499   Data is pooled from two replicates, statistical testing by ANOVA.

500   F. Ratio of R:S CFUs recovered from lck-/- ^{sa410} adult zebrafish infected with a mixture of

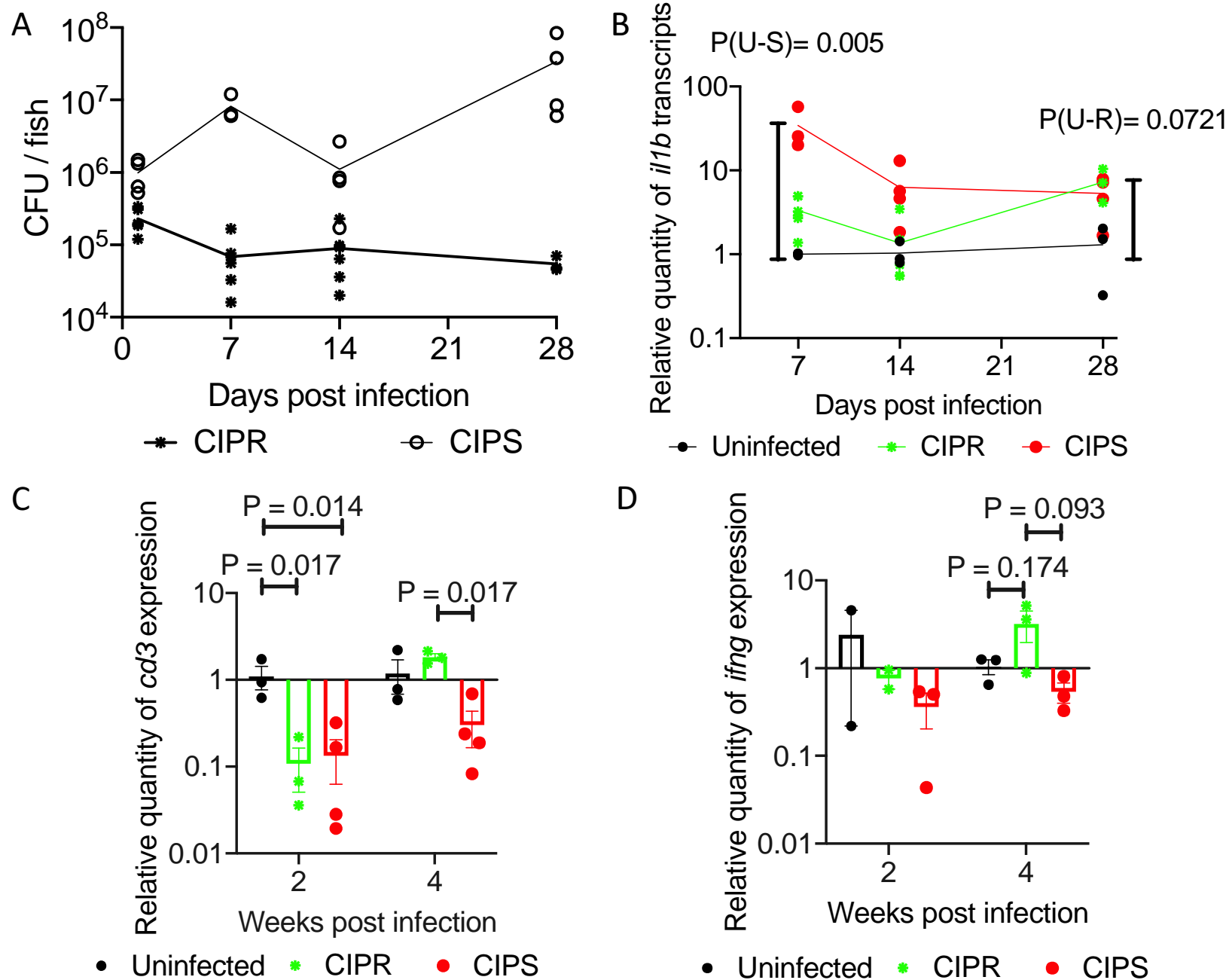501   differentially labelled R and S variants.

502

Figure 1
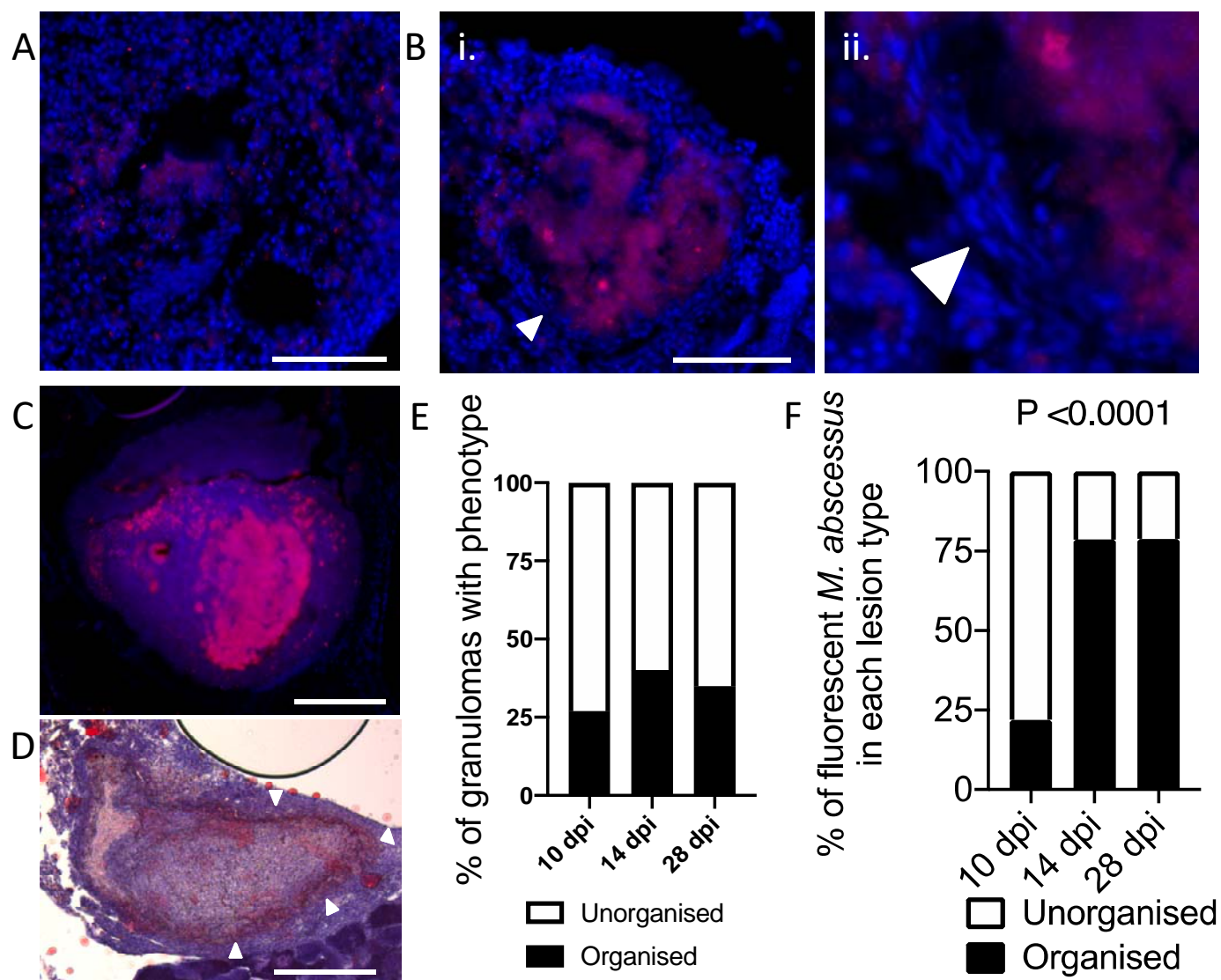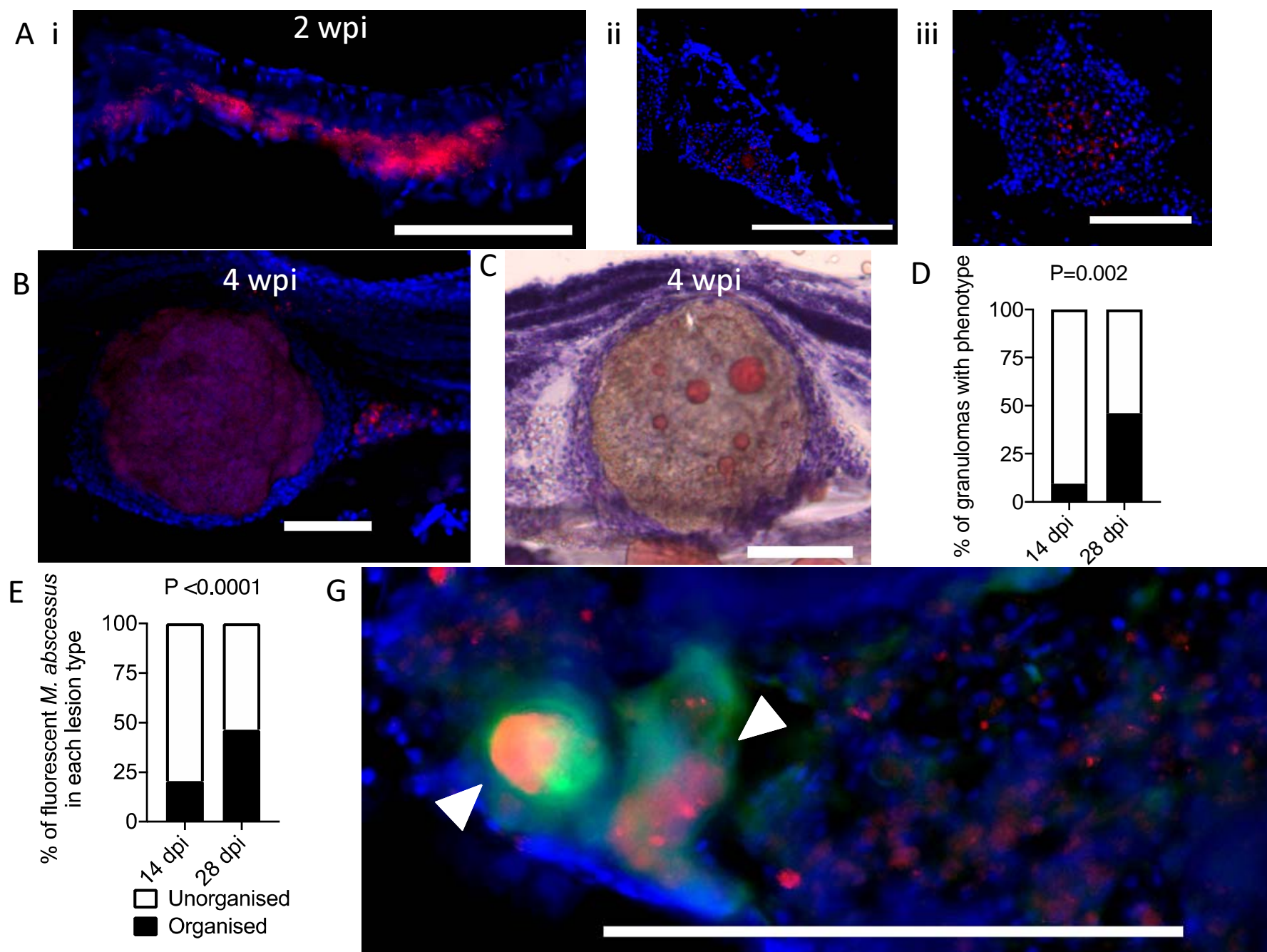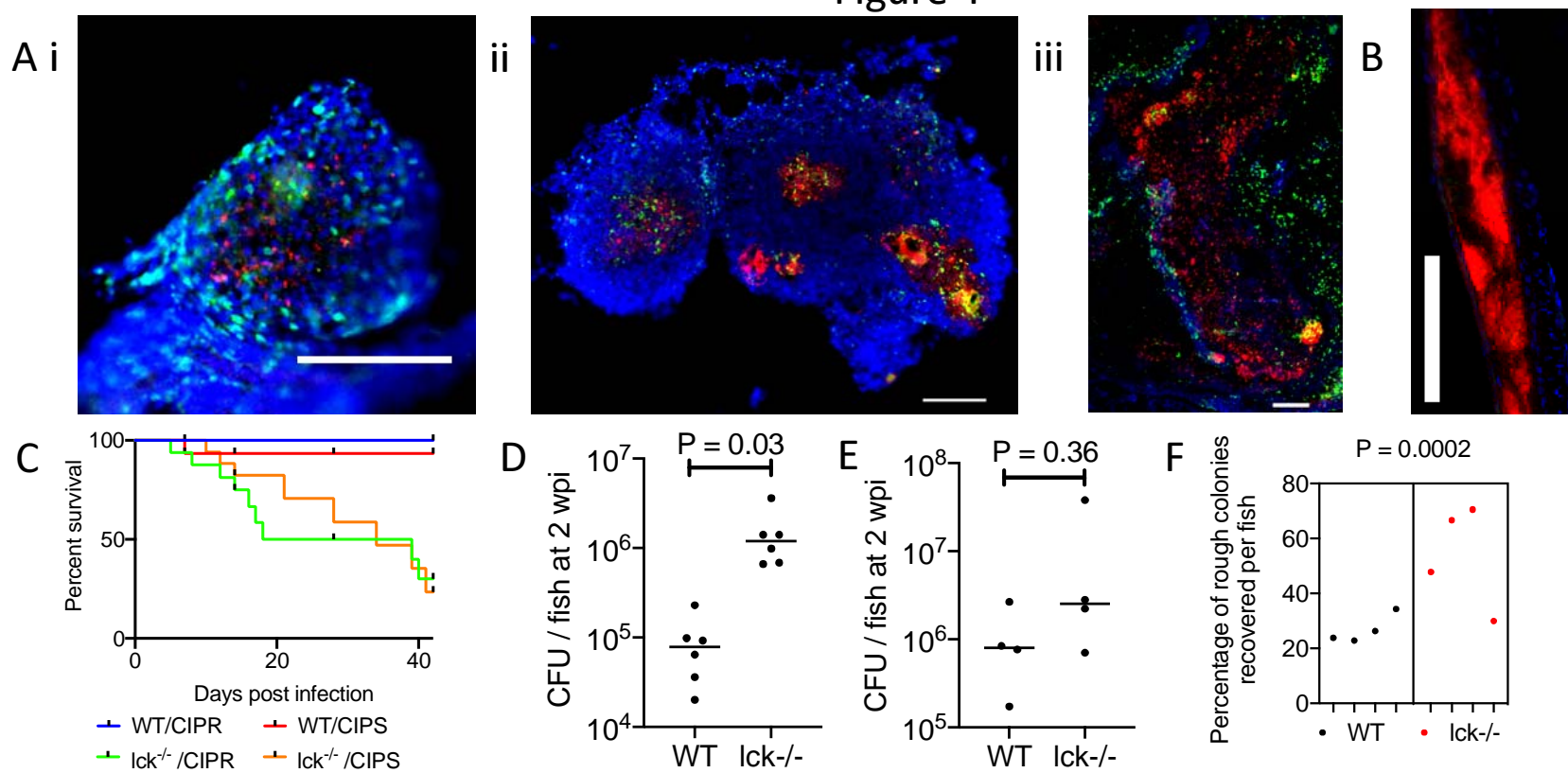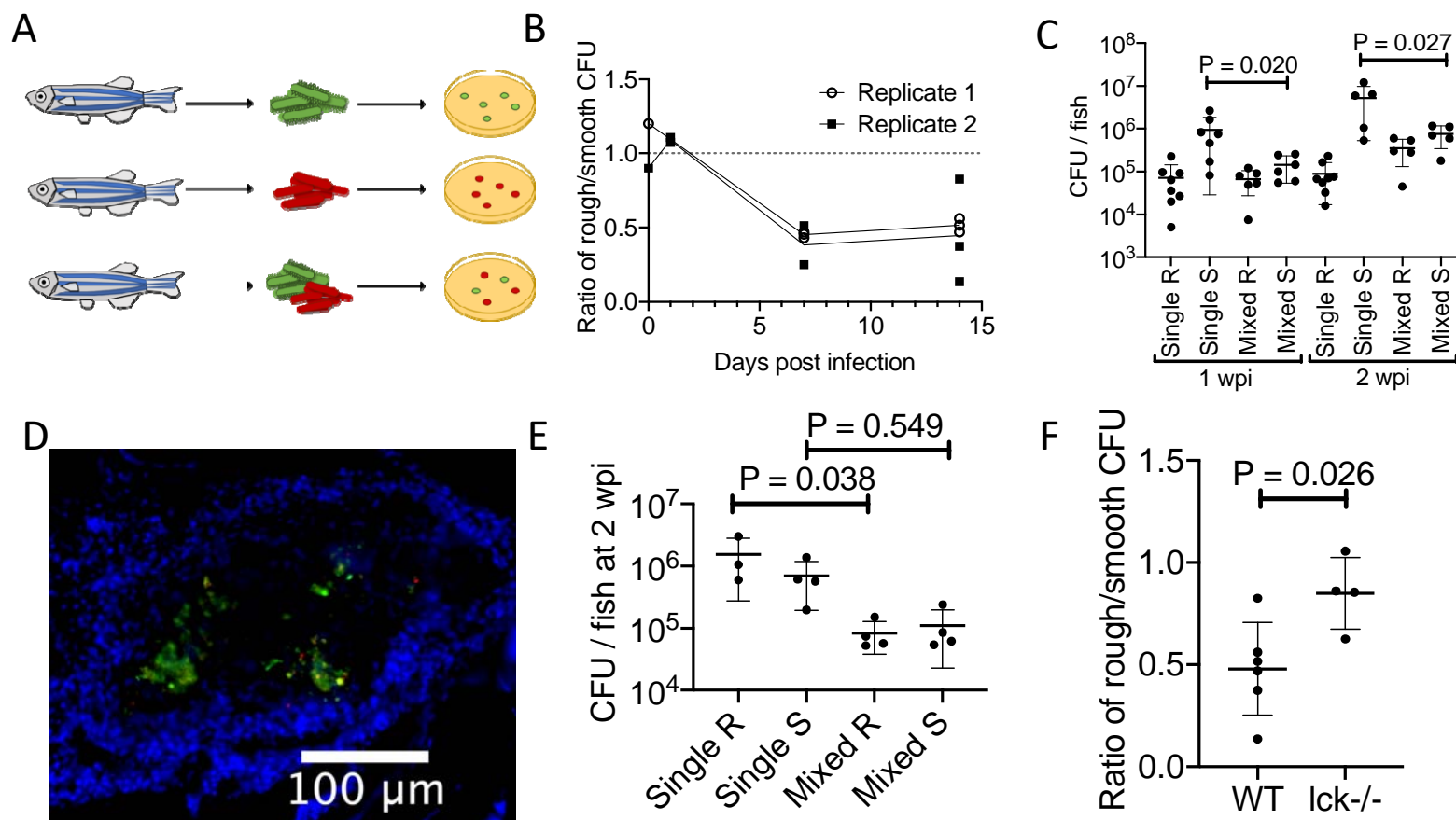
Figure 2

Figure 3

Figure 4

Figure 5

Graphical Abstract

Rough
M. abscessus

Smooth
M. abscessus

Controls

Activates

Controls

Adaptive immunity

Innate immunity